CellPress

How Slow RNA Polymerase II Elongation Favors Alternative Exon Skipping

Gwendal Dujardin,[1,2] Celina Lafaille,[1] Manuel de la Mata,[1,3] Luciano E. Marasco,[1] Manuel J. Muñoz,[1]
Catherine Le Jossic-Corcos,[2] Laurent Corcos,[2,4] and Alberto R. Kornblihtt[1,4,*]
[1]Laboratorio de Fisiología y Biología Molecular, Departamento de Fisiología, Biología Molecular y Celular, IFIBYNE-CONICET, Facultad de
Ciencias Exactas y Naturales, Universidad de Buenos Aires, Ciudad Universitaria, Pabellón 2, C1428EHA Buenos Aires, Argentina
[2]Inserm U1078-ECLA Team, Faculty of Medicine, 22 Avenue Camille Desmoulins, 29238 Brest Cedex 3, France
[3]Present address: Friedrich Miescher Institute for Biomedical Research, P.O. Box 2543, 4002 Basel, Switzerland
[4]Co-senior author
*Correspondence: ark@fbmc.fcen.uba.ar
http://dx.doi.org/10.1016/j.molcel.2014.03.044

SUMMARY

Splicing is functionally coupled to transcription, link-
ing the rate of RNA polymerase II (Pol II) elongation
and the ability of splicing factors to recognize splice
sites (ss) of various strengths. In most cases, slow
Pol II elongation allows weak splice sites to be recog-
nized, leading to higher inclusion of alternative exons.
Using CFTR alternative exon 9 (E9) as a model, we
show here that slowing down elongation can also
cause exon skipping by promoting the recruitment of
the negative factor ETR-3 onto the UG-repeat at E9
3′ splice site, which displaces the constitutive splicing
factor U2AF65 from the overlapping polypyrimidine
tract. Weakening of E9 5′ ss increases ETR-3 binding
at the 3′ ss and subsequent E9 skipping, whereas
strengthening of the 5′ ss usage has the opposite
effect. This indicates that a delay in the cotranscrip-
tional emergence of the 5′ ss promotes ETR-3 recruit-
ment and subsequent inhibition of E9 inclusion.

INTRODUCTION

Two different, but not exclusive, models have been proposed to
explain how transcription by RNA polymerase II (Pol II) regulates
alternative pre-mRNA splicing (Kornblihtt et al., 2013; Luco et al.,
2011). In the recruitment model, different splicing factors asso-
ciate with the transcription machinery or the chromatin template,
resulting in an increased concentration of these factors in the
vicinity of the pre-mRNA, regulating splicing choices (Das
et al., 2007; de la Mata and Kornblihtt, 2006; Huang et al.,
2012; Luco et al., 2010; Monsalve et al., 2000). In the kinetic
model, the rate of Pol II elongation influences the outcome of
alternative events (de la Mata et al., 2003; Kadener et al., 2001;
Roberts et al., 1998). The most frequent modality of alternative
splicing in mammals involves cassette exons that fail to be
included constitutively into mature mRNAs because they usually
possess suboptimal 3′ splice sites. The "first come, first served"
model explains how tandem arrays of a weak 3′ splice site
followed by a stronger one may lead to partial inclusion of the

alternative exon and how reduction in elongation rate can open
a time window for preferential inclusion of the upstream exon.
A direct proof for this model was provided by the use of mutant
forms of Pol II with a lower elongation rate. When transcription is
carried out by this slow polymerase, inclusion into mature mRNA
of the studied alternative cassette exons is greatly stimulated in
comparison to transcription by a wild-type enzyme (de la Mata
et al., 2003; Howe et al., 2003). Different factors and treatments
have been shown to modulate alternative splicing through the
control of Pol II elongation, for example, phosphorylation of the
transcribing polymerase (Ip et al., 2011; Muñoz et al., 2009), as-
sociation of Pol II to specific transcription factors (Close et al.,
2012; Nogués et al., 2002), and changes in DNA methylation
(Shukla et al., 2011), or in the chromatin template (Alló et al.,
2009; Ameyar-Zazoua et al., 2012; Nogués et al., 2002; Schor
et al., 2009, 2013). Although Pol II modifications could affect its
intrinsic kinetic behavior, covalent modifications of DNA and
histones would affect the chromatin structure, creating or elimi-
nating roadblocks to elongation. In both cases, differential
recruitment of elongation factors can also be involved. However,
several studies pointed to an integrative model for kinetic
coupling of splicing and transcription, where similar elongation
changes could promote different splicing outcomes (Dutertre
et al., 2010; Ip et al., 2011; Muñoz et al., 2009; Solier et al.,
2010). These genome-wide or multiple alternative splicing
event (ASE) analyses revealed that, contrary to the simplest
interpretation of the first come, first served mechanism (i.e.,
slow elongation causing high exon inclusion), a substantial part
of the modified ASEs displayed an increase in exon skipping.
To investigate the mechanism by which slow elongation pro-
motes exon skipping, we use the well-characterized alternative
exon 9 (E9) of the CFTR gene as a model. Our results show
that slow Pol II elongation promotes E9 skipping through the
recruitment of the negative splicing factor ETR-3 onto the uridine
and guanosine (UG) repeat located at intron 8 3′ end. To prove
this, we used several independent tools and treatments,
including transcriptional activators with differential elongation-
promoting activities, drugs affecting elongation such as
camptothecin (CPT) and 5,6-dichloro-1-beta-D-ribofuranosyl-
benzimidazole (DRB), UV irradiation, and a slow mutant of Pol
II. Using RNA immunoprecipitation (RNA-IP), we demonstrate
that, by promoting the binding of ETR-3 to its UG repeat target
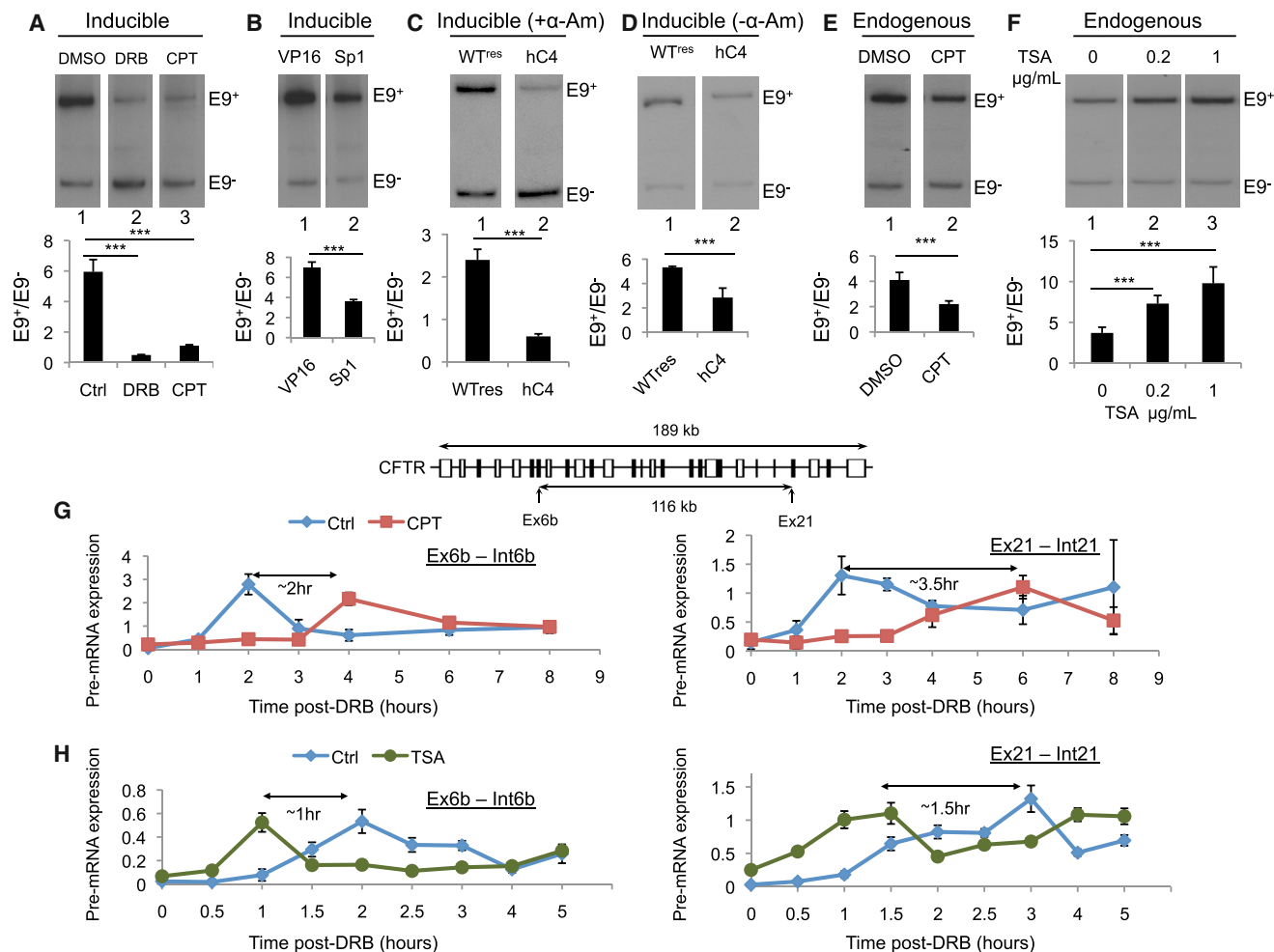
CrossMark

Figure 1. Slowing Down Transcription Elongation Rate Induces CFTR E9 Skipping
(A) HEK293T cells were cotransfected with the inducible E9 minigene and the VP16 transactivator and treated with DRB (50 μM) or CPT (6 μM) for 4 hr.
(B) HEK293T cells were cotransfected with the inducible E9 minigene and either the VP16 or the Sp1 transactivators.
(C) HEK293T cells were cotransfected with the inducible E9 minigene and expression vectors for WT[res] and hC4 Pol II followed by addition of α-amanitin.
(D) HEK293T cells were cotransfected with the inducible E9 minigene and expression vectors for WT[res] and hC4 Pol II without adding α-amanitin.
(E) Caco-2 cells were treated with DMSO or 1 μM CPT for 24 hr.
(F) Caco-2 cells were treated with TSA at the indicated concentration for 48 hr.
(G and H) Comparison of endogenous CFTR pre-mRNA expression measurement in the presence or absence of CPT 1 μM (G) or TSA 1 μg/ml[−1] (H).
(A–E) Radioactive RT-PCR analyses of CFTR E9 inclusion levels are shown. The histograms display ratios of radioactivity in E9+ and E9− bands are shown as means ± SD from at least three independent transfection experiments (***p < 0.001).

site, slow elongation stimulates the displacement of the constitutive splicing factor U2AF65 from the overlapping polypyrimidine tract of E9 3′ splice site (ss). Increased ETR-3 binding is dependent on poor E9 definition, suggesting that a delay in the cotranscriptional emergence of the 5′ ss prompts ETR-3 to bind more efficiently to its target site and inhibit E9 inclusion.

RESULTS

Inhibition of Pol II Elongation Increases CFTR E9 Skipping
To evaluate the impact of Pol II elongation rate on CFTR E9 ASE, we assessed the effects of drugs that inhibit transcription

elongation, such as DRB, a pTEF-b inhibitor, and camptothecin (CPT), a DNA topoisomerase I inhibitor (Boireau et al., 2007; Darzacq et al., 2007) that was previously shown to affect cotranscriptional splicing factor recruitment by inhibition of elongation (Listerman et al., 2006). We treated human embryonic kidney 293T (HEK293T) cells transfected with an inducible E9 alternative splicing reporter minigene with 6 μM CPT and 50 μM DRB, concentrations that do not completely inhibit transcription. Both DRB and CPT affected CFTR E9 splicing (Figure 1A), suggesting that inclusion of this exon follows the kinetic model of cotranscriptional splicing. However, and most interestingly, whereas the existing model postulates that slow elongation should induce exon inclusion, we observed exactly the opposite,

with an increase of exon skipping. To rule out side effects of the drugs, such as a decrease in splicing factor expression or activity, we decided to modulate the induction of transcription of the inducible minigene with two different transactivators: a transcription initiation activator (Sp1) and a transcription initiation and elongation activator (VP16), which is known to enhance the elongation rate (Blau et al., 1996; Nogués et al., 2002). As shown in Figure 1B, a fast elongation rate induced by the VP16 transactivator resulted in a better E9 inclusion level as shown by the higher $E9^+/E9^-$ ratio, which is in agreement with the previous result. Finally, a more direct way to analyze the effect of elongation rate on alternative splicing was the use of a slow Pol II mutant. For this, we cotransfected the E9 reporter minigene with a plasmid encoding an α-amanitin-resistant large subunit of Pol II (hC4) carrying a point mutation shown to slow elongation, measured in vivo and in real time, by 2- to 3-fold (Boireau et al., 2007). Consistently, when transcription is carried out by the slow polymerase CFTR E9, skipping is increased by 5-fold in comparison to the E9 inclusion levels under transcription by the α-amanitin-resistant wild-type polymerase (Figure 1C). A similar experiment performed without the addition of α-amanitin showed similar, although, as expected, quantitatively smaller, results (Figure 1D), ruling out a putative effect of this drug per se.

CPT Promotes Endogenous CFTR E9 Skipping

To validate the above results with the endogenous CFTR gene, we used the Caco-2 cell line, in which endogenous CFTR E9 is alternatively spliced, instead of HEK293T cells, where endogenous E9 inclusion is constitutive. Because of the limited transfection efficiency of Caco-2 cells, overexpression of the slow hC4 Pol II cannot be used to affect endogenous alternative splicing. Therefore, we decided to treat Caco-2 cells with CPT. Figure 1E shows that CPT is also effective to induce endogenous CFTR E9 skipping, although to a lesser extent than HEK293T cells transfected with the reporter minigene (Figure 1A). We reasoned that, if inhibition of Pol II elongation caused E9 skipping, then promotion of Pol II elongation should have the opposite effect. For this, we treated Caco-2 cells with the histone deacetylase inhibitor trichostatin A (TSA), which is known to create a more open chromatin structure that promotes elongation (Schor et al., 2009). Figure 1F shows that, as predicted, increasing concentrations of TSA promote E9 inclusion in the endogenous CFTR mRNA.

To be sure that the observed effects on splicing were due to an inhibition (CPT) or a promotion (TSA) of elongation, we compared Pol II elongation on the endogenous CFTR gene in the absence and presence of these drugs by reversibly blocking Pol II transcription with 300 μM DRB for 5 hr and subsequent washing off of DRB, allowing transcription to reinitiate, according to the procedure developed by Singh and Padgett (2009). We monitored the pre-mRNA levels through two RT-PCR amplicons, separated by 116 kbp, mapping at both sides of E9 at various times after DRB wash. As shown in Figure 1G, recovery of amplification was delayed for CPT-treated cells for both amplicons. Despite the long interval time-course used, because of the low CFTR gene expression in the Caco-2 cell line that did not allow us to calculate a precise speed of Pol II, we could observe an increment in the delay after CPT treatment between

E6b and E21 amplicons, indicating a decrease in Pol II elongation upon CPT treatment, validating our previous observations. Conversely, Figure 1H shows that TSA causes a faster recovery of transcription after the DRB wash at both amplicons, consistent with an increase in Pol II elongation rates. The mechanism through which CPT inhibits Pol II elongation is not known. Several groups have reported that CPT is able to induce Pol II hyperphosphorylation (Dutertre et al., 2010; Sordet et al., 2008). This was confirmed here by western blot (Figure S1A, top, available online), revealing a strong effect of phosphorylation of the large subunit of Pol II (Rpb1) after 1 hr of CPT treatment. This Pol II hyperphosphorylation is not accompanied by any qualitative or quantitative change in the abundance or phosphorylation of the SR proteins known to regulate E9 splicing (Figure S1A, bottom), which indicates that the changes in E9 splicing caused by CPT are not due to an effect of CPT on SR proteins. Because hyperphosphorylation of Rpb1 observed after UV irradiation was shown to be the cause of changes in alternative splicing because of a reduction in Pol II elongation (Muñoz et al., 2009), we decided to test the effects of both UV irradiation and transcription by Pol II phosphomimetic mutants on CFTR E9 splicing. As shown in Figures S1B and S1C, both UV irradiation and the phosphomimetic Pol II mutants, in which either Ser2 or Ser5 of Rpb1 CTD have been replaced by glutamic acid residues, induced E9 skipping, strengthening our observations. In order to validate that CFTR E9 responds in an opposite manner to elongation in the ASE model used to develop the kinetic model, we next analyzed the effect of CPT on fibronectin (FN) E33 (EDI) ASE. As hypothesized, CPT induced E33 inclusion (Figure S1D), demonstrating an opposite kinetic regulation of FN E33 and CFTR E9 ASEs.

It is worth pointing out that the effects on E9 splicing of all treatments shown in Figure 1 could be subject to alternative mechanistic explanations of pleiotropic nature. However, the fact that they all consistently give the expected results strengthens our confidence that they act through elongation. Under these premises, we next focused on understanding how slowing down elongation could induce exon skipping.

Direct Role of ETR-3 in the Kinetic Coupling

Three major intronic regulatory sequences of CFTR E9 ASE have been described: the UGmUn polymorphism at the end of intron 8, a polypyrimidine-rich controlling element (PCE), and an intronic splicing silencer (ISS) at the beginning of intron 9 (Chu et al., 1991; Pagani et al., 2000; Zuccato et al., 2004). In order to evaluate which of these sequences are implicated in the kinetic coupling, a panel of minigenes carrying different deletions (Figure 2A) was tested along with CPT treatment. Removal of the UG repeat induced almost full E9 inclusion and completely abolished the effect of CPT on E9 splicing (Figure 2B, lanes 3 and 4), suggesting a major role of the UG repeat, a sequence bound by the splicing factors TDP-43 and ETR-3 (Buratti et al., 2001; Dujardin et al., 2010), in the kinetic coupling of CFTR E9. Interestingly, deletion of the ISS also induced almost full E9 inclusion in absence of CPT (lane 5) but did not affect the CPT effect in bringing down E9 inclusion (lane 6). An opposite effect is observed with the ΔPCE minigene, where a dramatic drop in E9 inclusion is observed before treatment (lane 7) along with a
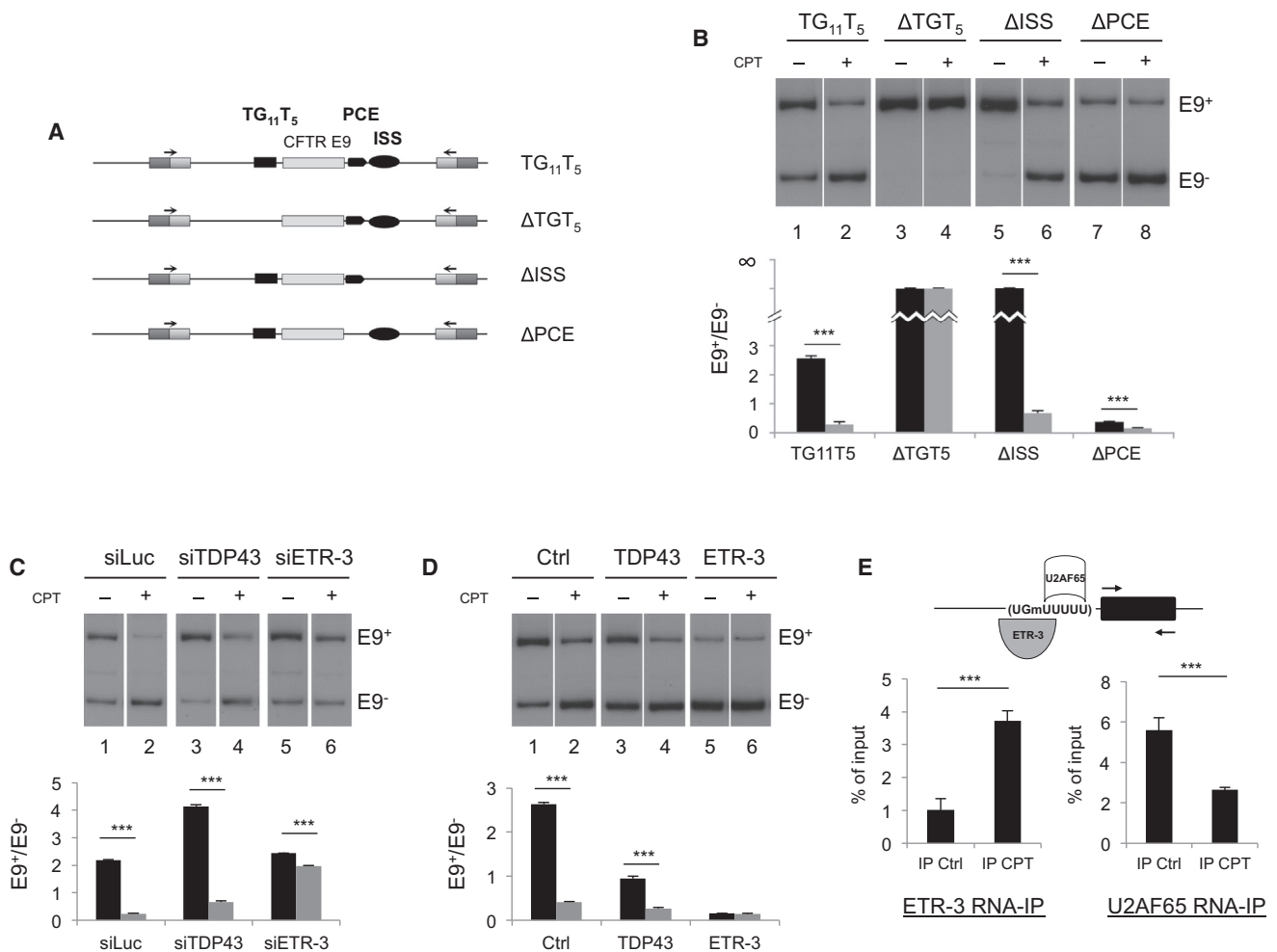
Figure 2. Role of ETR-3 in the Kinetic Cotranscriptional Splicing

(A) Representation of CFTR E9 reporter minigenes carrying deletions of the UG repeat (ΔTGT_5) of the ISS (ΔISS) or PCE (ΔPCE).

(B) HEK293T cells were transfected by the indicated minigene and treated with DMSO or CPT 6 μM for 4 hr.

(C and D) HEK293T cells were cotransfected with the $TG_{11}T_5$ minigene, indicated siRNA (C), or expression vector (D).

(E) Caco-2 cells were treated with DMSO or CPT 1 μM for 6 hr, and RNA-IP experiments were performed with an α-U2AF65 or α-ETR-3 antibody (***$p < 0.001$, n = 3).

Radioactive RT-PCR analyses of CFTR E9 inclusion levels are shown and quantified as in Figure 1.

much smaller effect of CPT on E9 skipping (lane 8). Similar results were obtained when, instead of CPT, the Sp1 transactivator was used to reduce elongation in comparison to the VP16 transactivator (Figure S2A). The ISS and PCE elements are thought to act in opposite ways by decreasing and increasing E9 5′ ss strength, respectively. According to these observations, results in Figure 2B suggest a role of the 5′ splice site in E9 splicing, independent of the elongation rate.

Focusing on the UGmUn sequence and to evaluate the role of TDP43 and ETR-3 in elongation control of E9 splicing, we performed small interfering RNA (siRNA)-mediated knockdown as well as overexpression of both splicing factors. Either knockdown (Figure 2C, lanes 3 and 4) or overexpression (Figure 2 D, lanes 3 and 4) of TDP-43 did not inhibit the increase in E9 skipping caused by CPT, indicating that TDP-43 is not involved in

the kinetic control of splicing. By contrast, both knockdown (Figure 2C, lanes 5 and 6) and overexpression (Figure 2D, lanes 5 and 6) of ETR-3 fully abolished the effect induced by CPT, strongly suggesting a major role of ETR-3 in the kinetic coupling. It is worth noting that similar results were observed with the use of the hC4 polymerase (Figure S2B).

One possible explanation for these results is that slow elongation favors recruitment of ETR-3 to its target site in the pre-mRNA, resulting in reduced E9 inclusion, by displacement of U2AF65, given that we have previously shown that both proteins compete in vitro for binding to the UGmUn polymorphism (Dujardin et al., 2010). This is also suggested by the proportional inhibition of the slow polymerase effect on E9 splicing with increasing amounts of ETR-3 (Figure S2C). To prove the hypothesis, we performed RNA-IP of both U2AF65 and ETR-3 on the
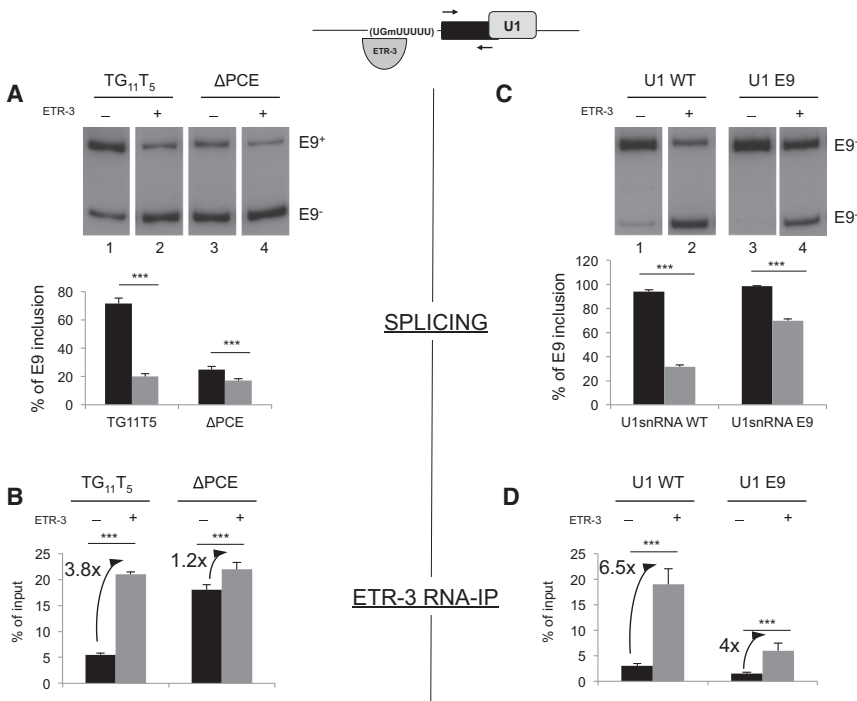
2). With ΔPCE as template, in which the 5′ ss is weakened, both E9 skipping and ETR-3 binding are much higher (compare lanes 1 and 3 of Figures 3A and 3B, respectively), and overexpression of ETR-3 has a smaller effect on both splicing and ETR-3 recruitment. These results suggest that, with a weak or not yet synthesized 5′ ss, binding of ETR-3 to the 3′ ss and E9 skipping are virtually maximal. To prove this mechanism through a different experimental approach, we took advantage of the intrinsically suboptimal sequence of CFTR E9 5′ss (aag/gua<u>g</u>uu versus the 5′ ss consensus nag/gur<u>a</u>gu). To increase the usage of this suboptimal 5′ss, we overexpressed a U1 small nuclear RNA (snRNA) that pairs perfectly with it (U1E9; Figure 3C) (Zuccato et al., 2004). As expected, U1E9 causes full E9 inclusion (lane 3) and reduces the effects of overexpressing ETR-3 on E9 inclusion by approximately 2-fold. This is paralleled at the ETR-3 recruitment level. Overexpression of U1E9 significantly reduces basal and overexpressed ETR-3 binding to its target site in the pre-mRNA (Figure 3D). Altogether, these results indicate that proper U1 small nuclear ribonucleic protein assembly is critical for preventing ETR-3 binding to the UGmUn polymorphism.

DISCUSSION

Here, we show that CFTR E9 alternative splicing is regulated by transcription through the control of Pol II elongation. Several treatments and tools that affect Pol II elongation rate also affect E9 inclusion (Figures 1A–1F, S1B, and S1C). Consistently, inhibition of histone deacetylation, previously shown to promote Pol II elongation (Schor et al., 2009), promotes E9 inclusion (Figure 1F). However, whereas the prevailing kinetic model links slow elongation to higher exon inclusion, we show that CFTR E9 inclusion displays an opposite correlation with elongation and unravel the underlying mechanism. We found that binding of the negative factor ETR-3, but not TDP-43, to the UG stretch at the end of intron 8 was responsible for increased E9 skipping (Figures 2B–2D) and that a slow Pol II elongation promotes ETR-3 binding and displacement of U2AF65 (Figure 2E). Furthermore, we provide evidence that increased ETR-3 binding is dependent on poor E9 definition. Our results strongly suggest that a delay in the cotranscriptional emergence of the 5′ ss would open a
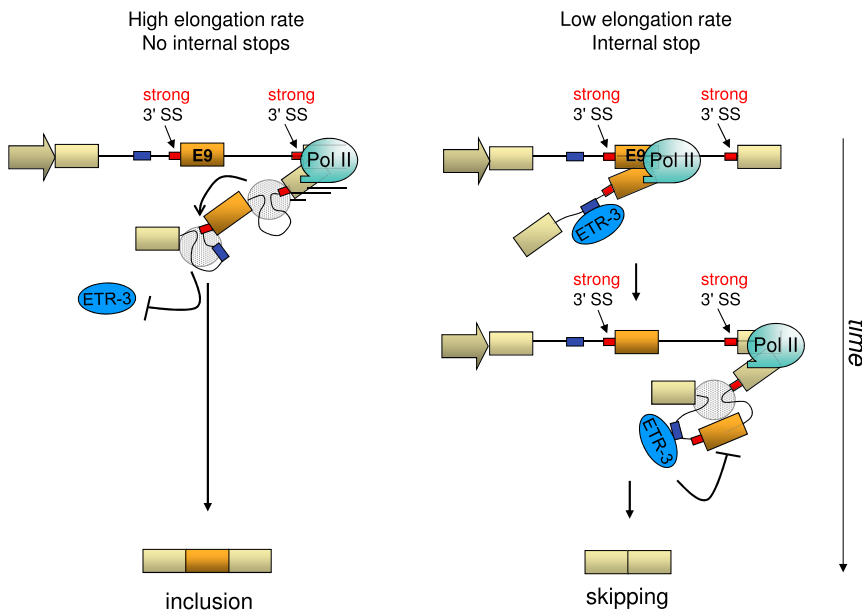
---

endogenous CFTR pre-mRNA after CPT treatment. Figure 2E shows that slowing down elongation with CPT increases the binding of ETR-3 to CFTR E9 3′ splice site (left) and displaces U2AF65 (right), which mechanistically explains the increase in E9 skipping. Similar effects were observed when transcription was carried out by the slow Pol II mutant (Figure S2D). Consistent with a key role for elongation, the use of TSA to increase elongation rates induced opposite effects to those of CPT and the slow Pol II; i.e., downregulation of ETR-3 binding and upregulation of U2AF65 binding (Figure S2E). As a control, CPT has no effect on the IP levels of TDP-43 (Figure S2F), confirming that, although its binding site partially overlaps with that of ETR-3, TDP43 is not involved in the kinetic control of E9 skipping.

Exon 9 Definition Is Critical for Kinetic Coupling

The fact that, although basal levels of E9 inclusion are affected when either the ISS or PCE elements are removed, CPT effects remain unaffected (Figure 2B) suggests a crosstalk between the UG repeat and the downstream 5′ ss in CFTR E9 splicing regulation, as previously proposed (Zuccato et al., 2004). We hypothesized that, because of this crosstalk, a delay in the synthesis of the 5′ ss could be responsible for the increase in ETR-3 recruitment to the 3′ ss caused by slow elongation. To evaluate this hypothesis, we assessed the effects of ETR-3 overexpression on both E9 splicing and ETR-3 binding to the UGmUn sequence with two different reporter minigenes with different 5′ ss strengths: TG$_{11}$T$_5$ and ΔPCE. The use of RNA-IP on minigene expression was first validated by immunoprecipitating recombinant tagged ETR-3 with an antitag Ab (Figure S3). Figure 3A shows that, with TG$_{11}$T$_5$ as template, ETR-3 overexpression promotes E9 skipping (Figure 3A, lanes 1 and 2) with concomitant increased binding to its target site (Figure 3B, lanes 1 and

Figure 4. Model of CFTR E9 Kinetic Coupling

The intronic sequence bound by the inhibitory splicing factor is represented by a dark blue box, the 3′ splice sites are depicted by red boxes, the CFTR alternative E9 is depicted by an orange box, and its two constitutive surrounding exons are depicted by yellow boxes. The spliceosome is represented by a gray circle. In the case of fast transcription elongation (left), ETR-3 does not bind the intronic sequence, exon definition takes place normally, and the CFTR E9 is included in the mRNA. In contrast, a slow elongation rate (right) gives a time window to ETR-3 to bind the intronic sequence before E9 definition and prevents spliceosome assembly to the E9 3′ ss, resulting in E9 skipping.

disease and cancer (David and Manley, 2010; Singh and Cooper, 2012), and many external physiological signals, as well as drugs, can reduce Pol II elongation rate, such as UV irradiation, for example (Boireau et al., 2007; Darzacq et al., 2007; Muñoz et al., 2009), and increase exon skipping.

EXPERIMENTAL PROCEDURES

Alternative Splicing Reporter Minigenes and Expression Vectors

The CFTR hybrid minigenes and the expression vectors for TDP-43 and ETR-3 have been described previously (Dujardin et al., 2010; Zuccato et al., 2004). To obtain the inducible pUHC-CFTR minigene, whose transcription is inactivated upon tetracycline treatment, we introduced a *Bst*EII site at the joint between α globin E3 and FN E32 of the pUHC-EDI minigene and replaced the *Bst*EII fragment with the *Bst*EII fragment from FN-CFTR in order to keep the same backbone between the two minigenes. Transcription of this minigene was induced by cotransfecting tetracycline-controlled transactivator (tTA)-Sp1 or (tTA)-VP16.

Pol II Expression Vectors

The expression vectors for α-amanitin-resistant variants of the large subunit of human Pol II (Rpb1) wild-type (WT[res]; pAT7Rpb1αAm[r] vector), and the hC4 mutant (pAT7Rpb1αAm[r]R749H) have been previously described (de la Mata et al., 2003). An α-amanitin-sensitive Rpb1 expression vector (WT[s]) was used as a control.

Cell Culture and Transfection

HEK293T and Caco-2 cells were grown in Dulbecco's modified Eagle's medium (DMEM) containing 4.5 g of glucose and DMEM-F12 (Lonza), respectively, and 10% fetal bovine serum (Gibco) at 37°C. Cells were plated at a density of 4.10^5 cells in 6-well plates 24 hr before transfection. Inducible minigene and Pol II transfections protocols have been previously described (de la Mata and Kornblihtt, 2006). Camptothecin 6 μM or DRB 50 μM were added after the tetracycline wash 4 hr before cell harvest. For noninducible minigenes, 1 μg of minigene was cotransfected with the same amount of ETR-3, U1-WT, U1-T9, or an empty vector. The day after, CPT 6 μM was added 4 hr before cell harvest. For siRNA experiments, cells were transfected with siLuc (5′-CUUACGCUGAGUACUUCGA-3′), siTDP-43 (5′-GCAAAGCCAAGAUGA GCCU-3′), or siETR-3 (5′-GGGUGAUGUUCUCUCCAUU-3′) at a final concentration of 20 nM. After 48 hr of transfection, CFTR hybrid minigene (1 μg) and the same amounts of siRNAs were transfected again, and cells were treated as mentioned above.

window of opportunity for ETR-3 to bind more efficiently to its target site and inhibit E9 inclusion. Although the actual delay caused by CPT at the E9 region is difficult to assess, one could speculate that, in the absence of CPT, and at an estimated 2 kb/min speed (Danko et al., 2013), it would take approximately 6 s for Pol II to transcribe the 200 bp that separate E9 3′and 5′ ss. Analysis of Pol II elongation by the Singh and Padgett (2009) method (Figure 1G) reveal significant delays of up to 3 hr in the recovery of CFTR pre-mRNA levels after the DRB wash in cells treated with CPT in comparison to nontreated cells. It should be noted that, because we are analyzing amplicons spanning splice junctions, the pre-mRNA levels measured are the consequence of both their recovery due to transcription and their disappearance due to splicing and/or RNA degradation. Assuming that these delays reflect a 3-fold reduction in overall elongation, the time needed by Pol II to transcribe E9 would go up to 18 s. Measurements of splicing kinetics have been obtained from in vitro splicing reactions (Darnell, 2013). Although there is little quantitative information about in vivo splicing kinetics, apart from the fact that most splicing takes place cotranscriptionally (Tilgner et al., 2012), in vivo imaging studies of cotranscriptional splicing revealed that the kinetics of splicing fits better with a mathematical model in which splicing occurs not at a single limiting step (assembly or catalysis) but three limiting steps, one of which occurs at the transcriptional elongation level (Schmidt et al., 2011). The model is consistent with the estimated rates for Pol II elongation (1.4–4 kb/min) (Boireau et al., 2007; Darzacq et al., 2007), but, most importantly, the model predicts that changes in elongation rates of about 2- to 3-fold, as observed in the present study, have a high impact on alternative splicing decisions if there are three limiting steps (kinetic coupling condition) in comparison to the assumption of only one limiting step.

Figure 4 summarizes our model for CFTR E9 kinetic splicing. The biological consequences of the mechanism described here are important because exon skipping is involved in genetic

RNA Extraction and RT-PCR

Total RNA was extracted with Tri-Reagent (Ambion) according to the manufacturer's instructions. One microgram of RNA was reverse transcribed with the M-MLV reverse transcriptase (Invitrogen) and oligo-dT primer, and the cDNA was amplified with primers α2-3 and B2 (Dujardin et al., 2010).

RNA-IP

In order to perform the RNA-IP, the iCLIP protocol was used (König et al., 2010) except that RNA was extracted by the addition of Tri-Reagent directly to the beads after the washing step. For the endogenous RNA-IP, Caco-2 cells were plated in 10 cm plates and treated the day after with 1 μM CPT for 6 hr. For the minigene RNA-IP, HEK293T cells plated in 10 cm plates and were transfected the day after with the indicated CFTR minigene, U1snRNA, and ETR-3 plasmids. For immunoprecipitation, 10 μg of α-U2AF65 (MC3, Sigma-Aldrich) or α-ETR-3 (1H2, Sigma-Aldrich) antibodies was used for each sample as well as a mouse control IgG (Santa Cruz Biotechnology). After RNA extraction, samples were treated with DNase I (Sigma-Aldrich) in order to prevent DNA contamination. RT reaction was initiated with random decamers, and cDNA was synthesized with SuperScript III RT (Invitrogen). Quantification of the pre-mRNAs was performed by real-time PCR with the E9F-RIP (AATGGTGATGA CAGCCTCTTCTTC) and E9R-RIP (ATCCAGCAACCGCCAACAAC) primers.

Pol II Elongation Measurement

An adaptation of the method developed by Singh and Padgett (2009) was used. A DRB treatment of 300 μM for 5 hr was necessary in order to fully block endogenous CFTR transcription. For the CPT-treated cells, CPT 1 μM was added 30 min before the DRB wash and remained until cell harvest. Total RNA was extracted as mentioned above. Reverse transcriptase reaction was initiated with random decamers. Quantification of the pre-mRNAs was performed by real-time PCR with amplicons spanning the intron-exon junctions. The primers used were Ex6bF (CAATCTGTTAAGGCATACTG), Ex6bR (AAATATGAGGTGGAAGTCTAC), Ex21F (ACCTATATGTCACAGAAGT), and Ex21R (AGTGTTCAGTAGTCTCAA). Results were expressed in relation to the pre-mRNA value of cells never treated with DRB.

SUPPLEMENTAL INFORMATION

Supplemental Information contains three figures and can be found with this article online at http://dx.doi.org/10.1016/j.molcel.2014.03.044.

REFERENCES

Alló, M., Buggiano, V., Fededa, J.P., Petrillo, E., Schor, I., de la Mata, M., Agirre, E., Plass, M., Eyras, E., Elela, S.A., et al. (2009). Control of alternative splicing through siRNA-mediated transcriptional gene silencing. Nat. Struct. Mol. Biol. 16, 717–724.

Ameyar-Zazoua, M., Rachez, C., Souidi, M., Robin, P., Fritsch, L., Young, R., Morozova, N., Fenouil, R., Descostes, N., Andrau, J.C., et al. (2012). Argonaute proteins couple chromatin silencing to alternative splicing. Nat. Struct. Mol. Biol. 19, 998–1004.

Blau, J., Xiao, H., McCracken, S., O'Hare, P., Greenblatt, J., and Bentley, D. (1996). Three functional classes of transcriptional activation domain. Mol. Cell. Biol. 16, 2044–2055.

Boireau, S., Maiuri, P., Basyuk, E., de la Mata, M., Knezevich, A., Pradet-Balade, B., Bäcker, V., Kornblihtt, A., Marcello, A., and Bertrand, E. (2007). The transcriptional cycle of HIV-1 in real-time and live cells. J. Cell Biol. 179, 291–304.

Buratti, E., Dörk, T., Zuccato, E., Pagani, F., Romano, M., and Baralle, F.E. (2001). Nuclear factor TDP-43 and SR proteins promote in vitro and in vivo CFTR exon 9 skipping. EMBO J. 20, 1774–1784.

Chu, C.S., Trapnell, B.C., Murtagh, J.J., Jr., Moss, J., Dalemans, W., Jallat, S., Mercenier, A., Pavirani, A., Lecocq, J.P., Cutting, G.R., et al. (1991). Variable deletion of exon 9 coding sequences in cystic fibrosis transmembrane conductance regulator gene mRNA transcripts in normal bronchial epithelium. EMBO J. 10, 1355–1363.

Close, P., East, P., Dirac-Svejstrup, A.B., Hartmann, H., Heron, M., Maslen, S., Chariot, A., Söding, J., Skehel, M., and Svejstrup, J.Q. (2012). DBIRD complex integrates alternative mRNA splicing with RNA polymerase II transcript elongation. Nature 484, 386–389.

Danko, C.G., Hah, N., Luo, X., Martins, A.L., Core, L., Lis, J.T., Siepel, A., and Kraus, W.L. (2013). Signaling pathways differentially affect RNA polymerase II initiation, pausing, and elongation rate in cells. Mol. Cell 50, 212–222.

Darnell, J.E., Jr. (2013). Reflections on the history of pre-mRNA processing and highlights of current knowledge: a unified picture. RNA 19, 443–460.

Darzacq, X., Shav-Tal, Y., de Turris, V., Brody, Y., Shenoy, S.M., Phair, R.D., and Singer, R.H. (2007). In vivo dynamics of RNA polymerase II transcription. Nat. Struct. Mol. Biol. 14, 796–806.

Das, R., Yu, J., Zhang, Z., Gygi, M.P., Krainer, A.R., Gygi, S.P., and Reed, R. (2007). SR proteins function in coupling RNAP II transcription to pre-mRNA splicing. Mol. Cell 26, 867–881.

David, C.J., and Manley, J.L. (2010). Alternative pre-mRNA splicing regulation in cancer: pathways and programs unhinged. Genes Dev. 24, 2343–2364.

de la Mata, M., and Kornblihtt, A.R. (2006). RNA polymerase II C-terminal domain mediates regulation of alternative splicing by SRp20. Nat. Struct. Mol. Biol. 13, 973–980.

de la Mata, M., Alonso, C.R., Kadener, S., Fededa, J.P., Blaustein, M., Pelisch, F., Cramer, P., Bentley, D., and Kornblihtt, A.R. (2003). A slow RNA polymerase II affects alternative splicing in vivo. Mol. Cell 12, 525–532.

Dujardin, G., Buratti, E., Charlet-Berguerand, N., Martins de Araujo, M., Mbopda, A., Le Jossic-Corcos, C., Pagani, F., Ferec, C., and Corcos, L. (2010). CELF proteins regulate CFTR pre-mRNA splicing: essential role of the divergent domain of ETR-3. Nucleic Acids Res. 38, 7273–7285.

Dutertre, M., Sanchez, G., De Cian, M.C., Barbier, J., Dardenne, E., Gratadou, L., Dujardin, G., Le Jossic-Corcos, C., Corcos, L., and Auboeuf, D. (2010). Cotranscriptional exon skipping in the genotoxic stress response. Nat. Struct. Mol. Biol. 17, 1358–1366.

Howe, K.J., Kane, C.M., and Ares, M., Jr. (2003). Perturbation of transcription elongation influences the fidelity of internal exon inclusion in Saccharomyces cerevisiae. RNA 9, 993–1006.

Huang, Y., Li, W., Yao, X., Lin, Q.J., Yin, J.W., Liang, Y., Heiner, M., Tian, B., Hui, J., and Wang, G. (2012). Mediator complex regulates alternative mRNA processing via the MED23 subunit. Mol. Cell 45, 459–469.

Ip, J.Y., Schmidt, D., Pan, Q., Ramani, A.K., Fraser, A.G., Odom, D.T., and Blencowe, B.J. (2011). Global impact of RNA polymerase II elongation inhibition on alternative splicing regulation. Genome Res. 21, 390–401.

Kadener, S., Cramer, P., Nogués, G., Cazalla, D., de la Mata, M., Fededa, J.P., Werbajh, S.E., Srebrow, A., and Kornblihtt, A.R. (2001). Antagonistic effects of

T-Ag and VP16 reveal a role for RNA pol II elongation on alternative splicing. EMBO J. *20*, 5759–5768.

König, J., Zarnack, K., Rot, G., Curk, T., Kayikci, M., Zupan, B., Turner, D.J., Luscombe, N.M., and Ule, J. (2010). iCLIP reveals the function of hnRNP particles in splicing at individual nucleotide resolution. Nat. Struct. Mol. Biol. *17*, 909–915.

Kornblihtt, A.R., Schor, I.E., Alló, M., Dujardin, G., Petrillo, E., and Muñoz, M.J. (2013). Alternative splicing: a pivotal step between eukaryotic transcription and translation. Nat. Rev. Mol. Cell Biol. *14*, 153–165.

Listerman, I., Sapra, A.K., and Neugebauer, K.M. (2006). Cotranscriptional coupling of splicing factor recruitment and precursor messenger RNA splicing in mammalian cells. Nat. Struct. Mol. Biol. *13*, 815–822.

Luco, R.F., Pan, Q., Tominaga, K., Blencowe, B.J., Pereira-Smith, O.M., and Misteli, T. (2010). Regulation of alternative splicing by histone modifications. Science *327*, 996–1000.

Luco, R.F., Alló, M., Schor, I.E., Kornblihtt, A.R., and Misteli, T. (2011). Epigenetics in alternative pre-mRNA splicing. Cell *144*, 16–26.

Monsalve, M., Wu, Z., Adelmant, G., Puigserver, P., Fan, M., and Spiegelman, B.M. (2000). Direct coupling of transcription and mRNA processing through the thermogenic coactivator PGC-1. Mol. Cell *6*, 307–316.

Muñoz, M.J., Pérez Santangelo, M.S., Paronetto, M.P., de la Mata, M., Pelisch, F., Boireau, S., Glover-Cutter, K., Ben-Dov, C., Blaustein, M., Lozano, J.J., et al. (2009). DNA damage regulates alternative splicing through inhibition of RNA polymerase II elongation. Cell *137*, 708–720.

Nogués, G., Kadener, S., Cramer, P., Bentley, D., and Kornblihtt, A.R. (2002). Transcriptional activators differ in their abilities to control alternative splicing. J. Biol. Chem. *277*, 43110–43114.

Pagani, F., Buratti, E., Stuani, C., Romano, M., Zuccato, E., Niksic, M., Giglio, L., Faraguna, D., and Baralle, F.E. (2000). Splicing factors induce cystic fibrosis transmembrane regulator exon 9 skipping through a nonevolutionary conserved intronic element. J. Biol. Chem. *275*, 21041–21047.

Roberts, G.C., Gooding, C., Mak, H.Y., Proudfoot, N.J., and Smith, C.W. (1998). Co-transcriptional commitment to alternative splice site selection. Nucleic Acids Res. *26*, 5568–5572.

Schmidt, U., Basyuk, E., Robert, M.C., Yoshida, M., Villemin, J.P., Auboeuf, D., Aitken, S., and Bertrand, E. (2011). Real-time imaging of cotranscriptional splicing reveals a kinetic model that reduces noise: implications for alternative splicing regulation. J. Cell Biol. *193*, 819–829.

Schor, I.E., Rascovan, N., Pelisch, F., Alló, M., and Kornblihtt, A.R. (2009). Neuronal cell depolarization induces intragenic chromatin modifications affecting NCAM alternative splicing. Proc. Natl. Acad. Sci. USA *106*, 4325–4330.

Schor, I.E., Fiszbein, A., Petrillo, E., and Kornblihtt, A.R. (2013). Intragenic epigenetic changes modulate NCAM alternative splicing in neuronal differentiation. EMBO J. *32*, 2264–2274.

Shukla, S., Kavak, E., Gregory, M., Imashimizu, M., Shutinoski, B., Kashlev, M., Oberdoerffer, P., Sandberg, R., and Oberdoerffer, S. (2011). CTCF-promoted RNA polymerase II pausing links DNA methylation to splicing. Nature *479*, 74–79.

Singh, R.K., and Cooper, T.A. (2012). Pre-mRNA splicing in disease and therapeutics. Trends Mol. Med. *18*, 472–482.

Singh, J., and Padgett, R.A. (2009). Rates of in situ transcription and splicing in large human genes. Nat. Struct. Mol. Biol. *16*, 1128–1133.

Solier, S., Barb, J., Zeeberg, B.R., Varma, S., Ryan, M.C., Kohn, K.W., Weinstein, J.N., Munson, P.J., and Pommier, Y. (2010). Genome-wide analysis of novel splice variants induced by topoisomerase I poisoning shows preferential occurrence in genes encoding splicing factors. Cancer Res. *70*, 8055–8065.

Sordet, O., Larochelle, S., Nicolas, E., Stevens, E.V., Zhang, C., Shokat, K.M., Fisher, R.P., and Pommier, Y. (2008). Hyperphosphorylation of RNA polymerase II in response to topoisomerase I cleavage complexes and its association with transcription- and BRCA1-dependent degradation of topoisomerase I. J. Mol. Biol. *381*, 540–549.

Tilgner, H., Knowles, D.G., Johnson, R., Davis, C.A., Chakrabortty, S., Djebali, S., Curado, J., Snyder, M., Gingeras, T.R., and Guigó, R. (2012). Deep sequencing of subcellular RNA fractions shows splicing to be predominantly co-transcriptional in the human genome but inefficient for lncRNAs. Genome Res. *22*, 1616–1625.

Zuccato, E., Buratti, E., Stuani, C., Baralle, F.E., and Pagani, F. (2004). An intronic polypyrimidine-rich element downstream of the donor site modulates cystic fibrosis transmembrane conductance regulator exon 9 alternative splicing. J. Biol. Chem. *279*, 16980–16988.